

Accepted Manuscript

Title: Preparation and characterisation of novel chlorothiazide potassium solid-state salt forms: intermolecular self assembly suprastructures.

Authors: Krzysztof J. Paluch, Lidia Tajber, Thomas McCabe, John E. O'Brien, Owen I. Corrigan, Anne Marie Healy



PII: S0928-0987(10)00388-X
DOI: doi:10.1016/j.ejps.2010.11.012
Reference: PHASCI 2171

To appear in: *European Journal of Pharmaceutical Sciences*

Received date: 22-9-2010
Revised date: 9-11-2010
Accepted date: 22-11-2010

Please cite this article as: Paluch, K.J., Tajber, L., McCabe, T., O'Brien, J.E., Corrigan, O.I., Healy, A.M., Preparation and characterisation of novel chlorothiazide potassium solid-state salt forms: intermolecular self assembly suprastructures., *European Journal of Pharmaceutical Sciences* (2010), doi:10.1016/j.ejps.2010.11.012

This is a PDF file of an unedited manuscript that has been accepted for publication. As a service to our customers we are providing this early version of the manuscript. The manuscript will undergo copyediting, typesetting, and review of the resulting proof before it is published in its final form. Please note that during the production process errors may be discovered which could affect the content, and all legal disclaimers that apply to the journal pertain.

**Preparation and characterisation of novel chlorothiazide potassium solid-state salt forms:
intermolecular self assembly suprastructures.**

Krzysztof J. Paluch^a, *Lidia Tajber*^a, *Thomas McCabe*^b, *John E. O'Brien*^b, *Owen I. Corrigan*^a,
Anne Marie Healy^{a*}

a) School of Pharmacy and Pharmaceutical Sciences, b) School of Chemistry

Trinity College Dublin, College Green, Dublin 2, Ireland.

* To whom correspondence should be sent. Ph.: 00 353 1896 1444, e-mail: healyam@tcd.ie

Abstract:

Chlorothiazide (CTZ) is a poorly soluble diuretic agent. The aim of the present work was to produce and characterise a potassium salt form of chlorothiazide which has the potential advantages of improved aqueous solubility and potassium supplementation. A number of novel potassium salt forms of CTZ (CTZK) were prepared: CTZK monohydrate (form I), CTZK dihydrate (form II), anhydrous CTZK (form III), CTZK monohydrate hemimethanolate (form IV) and a desolvate of CTZK monohydrate hemimethanolate (form V). These salt forms were characterised by thermal analysis, PXRD, NMR, elemental analysis, FTIR, Karl Fisher titrimetry, ICP-MS and GC-MS. The ethanol-free CTZK forms were also characterised by dynamic vapour sorption analysis (DVS). CTZK form I was stable (in the DVS) over the range 0% to 60% RH. The dihydrate form of the salt was stable (in the DVS) over a broader range of relative humidities, 10 to 90%RH at 25°C. CTZK form II was less hygroscopic at high humidities (70-90% RH) than the previously reported CTZNa dihydrate. Single crystal X-ray analysis indicated that chlorothiazide potassium, crystallised from water or water/acetone mixture, formed a dihydrated polymeric-like intermolecular self-assembly (ISA) suprastructure. The ISA coordination was determined to be: $(\text{CTZ})_3 \cdot \text{K} \cdot (\text{H}_2\text{O})_2 (\text{CTZ})_2 \cdot (\text{H}_2\text{O})_2 \cdot \text{K} \cdot (\text{CTZ})_3$ (monoclinic, space group: C2/c, single crystal cell parameters: $a = 18.328(4) \text{ \AA}$, $b = 7.3662(16) \text{ \AA}$, $c = 19.993(5) \text{ \AA}$, $\alpha = 90^\circ$, $\beta = 99.729(3)^\circ$, $\gamma = 90^\circ$). When CTZK was crystallised from ethanol, a monohydrate hemimethanolate ISA was formed, described as $(\text{CTZ})_3 \cdot \text{K} \cdot \text{CTZ} \cdot (\text{H}_2\text{O})_2 \cdot \text{CTZ} \cdot \text{K} \cdot (\text{CTZ})_2$ (triclinic, space group: P-1, single crystal cell parameters: $a = 7.078(3) \text{ \AA}$, $b = 9.842(5) \text{ \AA}$, $c = 21.994(11) \text{ \AA}$, $\alpha = 87.522(13)^\circ$, $\beta = 84.064(14)^\circ$, $\gamma = 78.822(12)^\circ$). The aqueous solubility of CTZK dihydrate, was determined to be $78.71 \pm 1.82 \text{ mg/ml}$, approximately 400-fold higher than chlorothiazide, indicating a biopharmaceutical advantage associated with the potassium salt form.

Key words

Chlorothiazide potassium, Calorimetry (DSC), Crystal structure, Solvate, Moisture sorption, NMR spectroscopy, Solid state characteristics

1. Introduction

Approximately 40% of active pharmaceutical ingredients (API) are described as having poor aqueous solubility (Wu and Benet, 2005) and therefore are classified as classes II and IV of the Biopharmaceutics Classification System. There is great interest in the optimisation of the physicochemical properties of APIs, leading to an improved solubility of material and therefore improved bioavailability (Blagden et al., 2007). One of the main solubility enhancement approaches employed for ionisable drugs is salt formation (Stahl and Wermuth, 2008).

It is known that increasing hydrophilicity and decreasing melting point can result in the formation of a salt with increased aqueous solubility. Other desirable physicochemical properties include low hygroscopicity, physical stability of the crystal form under different storage conditions and chemical stability.

The salt formers (counterions) may be chosen from a few classes. The first class of salt-formers have unrestricted use for this purpose because they form physiologically ubiquitous ions (e.g. Cl^- , Na^+ , K^+) or because they occur as intermediate metabolites in biochemical pathways (e.g. citrate, glucuronate). Nearly 90% of the reported pharmaceutical salts are with sodium, calcium, potassium, magnesium, meglumine or ammonia with more than 55% made with sodium cations (Stahl and Wermuth, 2008). Pharmaceutical salts of potassium are less frequent in comparison to sodium salts. However, there are reports outlining several advantages of potassium over sodium salts. Sodium forms hydrated salts more readily than the potassium cation and the latter are less deliquescent than the sodium counterparts (Remington, 2005), e.g. the potassium salt of penicillin G is preferred to the sodium salt because it is less hygroscopic (Swarbrick, 2007). Potassium salts may have better aqueous solubility than the corresponding sodium salts (Derry et al., 2009, Adams et al., 2000, Antoncic and Copar, 2009).

Chlorothiazide (CTZ) is a thiazide diuretic which is administered orally in the crystalline form as tablets or as an oral suspension (Brunton et al., 1996). CTZ has a particularly high melting point ($\sim 350^\circ\text{C}$ with degradation) (Paluch et al. 2010). It is very slightly soluble in water, but readily soluble in

aqueous alkali solutions (European Pharmacopoeia, 2007), which is as a result of its acidic properties, allowing salt formation due to its salt-forming properties and taking into account the drug's poor solubility, it is considered advantageous to prepare a more soluble form. CTZ is available as a sodium salt, marketed as Diuril Sodium[®], however the solid-state properties of chlorothiazide sodium have only recently been presented (Paluch et al., 2010). Thiazides are considered to be effective antihypertensives, used as front-line drugs to treat hypertension (Appel, 2002). As with other thiazides, one limitation of the therapeutic use of CTZ is the risk of hypokalemia and the requirement for potassium supplementation (Ellison and Loffing, 2009). Thus the delivery of a potassium salt of CTZ may, first of all, have clinical advantages and furthermore, an improved solubility leading to an enhanced dissolution and potentially bioavailability. Therefore the main aim of this paper was to establish the conditions of preparation of a potassium salt of CTZ and characterise any salt products formed.

2. Materials and methods

2.1. Materials

Materials used in experiments were chlorothiazide (CTZ) obtained from Sigma (Ireland), potassium hydroxide (KOH) from Merck (Germany) and potassium bromide (KBr, FT-IR grade) from Sigma (Ireland). The following solvents and other reagents were also used including deionised water obtained from Purite Prestige Analyst HP water purification system, acetone (analytical grade) from Corcoran Chemicals, ethanol ($H_2O < 0.1\%$) from Corcoran Chemicals, methanol HPLC grade from Sigma (Ireland), deuterated dimethyl sulphoxide (DMSO- D_6) from Apollo Scientific Limited (UK), hydrogen peroxide (H_2O_2 , Ph. Eur., B.P. 30%) from Riedel de Haën (Germany), formic acid (HPLC grade) from Sigma (Ireland), nitric acid (HNO_3 , 69%, Aristar) from BDH (UK), hydrochloric acid 32% (HCl, extra pure) from Riedel de Haën (Germany) and Hydranal-Composite from Riedel de Haën (Germany).

2.2. Methods

2.2.1. Sample preparation

Chlorothiazide potassium (CTZK) was prepared by mixing chlorothiazide powder with 1M KOH aqueous solution. The product was then treated as described earlier (Paluch et al. 2010). This gave a white powder (hereafter referred to as form I). The crystals subsequently used for single crystal X-ray and other analyses were prepared by solvent evaporation from saturated solutions under constant nitrogen flow at room temperature (20°C-23°C). CTZK crystals were obtained by evaporation of water or 1:1 acetone/water mixture (both referred to as form II) or ethanol (referred to as form IV). A desolvated form IV was obtained by additional drying of crystals at 80°C for 24 hours and this material is referred to as form V. The anhydrous form III of CTZK was prepared by additional drying in the thermogravimetric analyser (TGA) of form I using the following temperature programme: 25°C-180°C-25°C with a heating/cooling rate of 10°C/min.

2.2.2. Analytical methods

Prepared materials were subsequently characterised using: powder X-ray diffraction (PXRD), differential scanning calorimetry (DSC), thermogravimetric analysis (TGA), Karl Fischer titrimetry, solid state Fourier transform infrared spectroscopy (FTIR), elemental analysis, dynamic vapour sorption (DVS), nuclear magnetic resonance (^1H NMR, ^{13}C NMR), inductively coupled plasma–mass spectrometry (ICP-MS) and solubility studies as described earlier (Paluch et al. 2010).

Scanning electron microscopy (SEM) was performed using a Tescan Mira Variable Pressure Field Emission Scanning Electron Microscope. Resolution: 3 nm at 30 kV, accelerating voltage: 5 kV, specimen stage: 300 mm by 330 mm (Compucentric), detector: secondary electron. Samples were glued onto aluminium stubs and sputter-coated with gold under vacuum prior to analysis.

Gas chromatography – mass spectrometry (GC-MS) was performed on a Varian 3800 Gas Chromatograph coupled with the Varian Saturn 2200 Ion Trap Mass Spectrometer (GC-MS). Ethanol eluted at 8.1 minutes and acetone at 8.7 minutes. The column used for the analysis was a WCOT fused Silica 60m x 0.32mm ID coating CP-SELECT 624 CB DF=1.8.

The data sets for crystals of CTZK were collected on a Rigaku Saturn 724 CCD diffractometer (Paluch et al. 2010). Suitable crystals of each compound were selected and mounted using inert oil on a 0.30 mm quartz fibre tip and immediately placed on the goniometer head in a 108-118K nitrogen gas stream.

The crystallographic data was analysed using: Mercury 2.2 (Blessing, 1995), Ortep-3 (Faruggia, 1997) and Platon (Spek, 2003) whereas the program Crystal Explorer 2.1 (McKinnon et al., 2004) was used to visualise and analyse Hirshfeld surfaces of molecules (Hirshfeld, 1977). The enhancement factor of 100% was used in all fingerprint plots to improve visualisation of interactions.

3. Results and discussion

3.1. Physicochemical analysis

Chlorothiazide potassium monohydrate, crystallised from water (form I), was a white crystalline powder. The DSC thermogram (Fig. 1e) of form I shows a small endotherm with an onset at around 58.0 ± 2.0 °C which corresponds to a loss of around $1.0 \pm 0.4\%$ of residual moisture by TGA (Fig. 1a), the second endotherm is related to the loss of hydrated water and has an onset at 160.6 ± 0.5 °C. The first event can be assigned to evaporation of loosely bound water and the second to liberation of water more tightly attached to the molecule of CTZK. The overall water loss corresponds to a $4.9 \pm 0.2\%$ mass loss (TGA) which, when converted to the molar ratio, indicates that 1 mole of CTZK contains one mole of water; thus form I is CTZ monohydrate. The theoretical calculation of water content in CTZK monohydrate is 5.1% w/w. This result was consistent with Karl Fischer titration which determined the water content to be $5.3 \pm 0.6\%$. Results of elemental analysis for CTZK form I were as follows: $23.58 \pm 0.1\%$ of carbon $1.86 \pm 0.05\%$ of hydrogen and $11.69 \pm 0.06\%$ of nitrogen, consistent with theoretical calculations for the monohydrate of: 23.90% of carbon, 2.01% of hydrogen and 11.94% of nitrogen.

The results of DSC/TGA analysis of CTZK form II (Fig. 1: b and f) differ from the results obtained for form I, as well as those for CTZK form IV (Fig. 1: c and g). CTZK form II (Fig. 1: b and f) presents two strong endotherms in the DSC scan, the first one starting immediately at the beginning of the scan (at 25 °C), corresponding to a TGA mass loss of $6.6 \pm 0.4\%$ detected between 25-100 °C and the second endotherm with an onset at 159.6 ± 0.5 °C corresponding to a TGA mass loss of $4.6 \pm 0.2\%$ (temperature range of 100-200 °C).

DSC and TGA analysis is consistent with CTZK form II being a dihydrate (theoretical water content of 9.7%), possibly containing interstitial/channel water molecule(s). For this sample the KF titrimetry indicated $13.4\% \pm 0.3\%$ of water content. This was higher than the mass loss determined by TGA analysis ($11.2 \pm 0.6\%$ measured between 25 and 200 °C), which may be attributed to different

sample handling conditions pertaining to the two techniques. Dehydration of this sample, occurring in two steps, was different to that of the sodium salt (CTZNa) dihydrate, which dehydrated in a single step (Paluch et al., 2010). Also, the onset of CTZNa dihydrate desolvation was 83.7 ± 0.5 °C, higher than that of the first endothermic event for CTZK form II indicating lower thermal stability of CTZK dihydrate. CTZK form II starts to melt at 263 ± 0.5 °C and this is immediately followed by decomposition. The potassium content was determined to be $12.5 \pm 0.6\%$ w/w, consistent with a 1:1 molar ratio of potassium to CTZ, where the theoretical content of potassium is 11.7%. The acetone content for the sample recrystallised from the acetone/water 1:1 (v/v) mixture was determined to be 3.0 ± 0.6 ppm.

The DSC scan of CTZ form IV (crystallised from ethanol) presents three endotherms with onsets at 35.4 ± 1.5 °C, 120.3 ± 1.2 °C (double endotherm) and 154.4 ± 0.6 °C. TGA showed a two step mass loss, one being $2.1 \pm 0.2\%$ (25-100 °C) and the other $11.3 \pm 1.0\%$ (100-200 °C). The ethanol content in the sample was $6.1 \pm 0.2\%$ as determined by GC-MS and consistent with the ethanol content of a monohydrate hemiethanolate of CTZ (i.e. CTZ:H₂O:ethanol of 1:1:0.5). The theoretical molar ratio corresponds to 6.1% w/w of ethanol and 4.8% w/w of water. This gives 10.9% total solvent content in the crystallised material, slightly lower than the total $13.4 \pm 2.0\%$ mass loss observed between 25-200 °C by TGA. The melting point of CTZK form IV is 272.0 ± 1.0 °C and the process of melting is followed by exothermic decomposition.

The pXRD pattern of CTZK form I and that of CTZK form IV (Fig. 2) are different in terms of peak positions indicating the different crystal form, which is not surprising considering the presence of ethanol in the latter material. Drying the crystals of CTZK form IV for 24 hours at 80 °C allowed the ethanol content to be reduced to 1.4 ± 0.4 ppm indicating that the ethanol molecules could easily be removed. It was confirmed by pXRD that the pattern of the dried sample showed a major change indicating modifications of the original crystal lattice. The diffraction peaks were reduced in intensity and the peak pattern was considered to be different to that of CTZK form IV (Fig. 2. a). Morphologically a difference could be noticed as transparent colourless hard crystals became white,

very fragile and formed a powder. Therefore the new form V is a desolvate originating from CTZK form IV and due to its distinctive X-ray powder pattern (Fig. 2 e), also different to that of the monohydrate form I (Fig. 2 b), it may be an alternative polymorphic form of the CTZK monohydrate. The diffraction pattern for CTZK form II (Fig. 2 c) was different to that of CTZK form I (Fig. 2 b). Additional drying of form I converted the monohydrate to an anhydrous form III. The pXRD pattern of the anhydrate (Fig. 2 d) is characterised by peaks having very low intensities with only one prominent peak at $19.85\ 2\theta$ suggesting major damage to the original crystal structure.

Investigations of the solid-state behaviour of CTZK imply that form II (dihydrate) is preferentially crystallised from an aqueous environment (water and water/acetone mixture studied). At ambient conditions over approximately 2-3 days, large crystals of this form were observed to lose their transparency and break apart from one another, converting to the form I (monohydrate), followed by the formation of the anhydrous form III when exposed to higher temperatures (over $160\ ^\circ\text{C}$). The latter is very sensitive to moisture and in humid conditions tends to recrystallise towards a mono and dihydrated form. Form IV (hemiethanolate) is recrystallised from ethanol, however at ambient conditions ethanol is progressively liberated and, depending on the environmental humidity and temperature, the desolvated CTZK forms a dihydrate, monohydrate or the anhydrous form III at a higher temperature.

To specify more precisely the humidity conditions which stabilise or induce transformation of the hydrate forms, CTZK form I (monohydrate) was subjected to dynamic vapour sorption analysis. An isothermal experiment of sorption and desorption at $25\ ^\circ\text{C}$ (Fig. 3) established that even $\sim 0\%$ RH (0.5-0.7% RH actual % RH) transformation of the monohydrate (I) towards an anhydrous form was not observed.

A sample of form I equilibrated at 0% RH remained stable as the monohydrate, in contrast to CTZNa, where the same conditions resulted in an anhydrous form (Paluch et al. 2010). CTZK recovered from the DVS experiment (after equilibration at 0% target RH) was analysed by pXRD (Fig. 4 f, g), and by thermal methods (Fig. 5.1a, 2a). The pXRD pattern was consistent with the pattern of CTZK monohydrate raw material (form I) described above (Fig. 2 b).

A sample of form I equilibrated up to 60% RH in 10% RH steps adsorbed less than 1% of water relative to the initial sample mass (CTZK monohydrate), indicating better moisture-related stability in comparison to CTZNa monohydrate, which was found to form *in situ* by DVS at 30-40% RH, rapidly absorbed water above 40% RH and recrystallised to a dihydrate (Paluch et al., 2010). The sample of CTZK recovered from the DVS instrument and subjected to thermal analysis presented a two stage mass loss, by TGA (Fig. 5. 2 f), the first of 3.44% and second of 5.47%, which correlated with two respective endothermal events on the DSC with onsets at 57.7°C and 142.5°C (Fig. 5 1 f). PXRD analysis of the sample equilibrated during sorption at 60% RH (Fig. 4 e) had a Bragg peaks pattern which was very similar to that of the monohydrate form I but with the appearance of additional peaks, in particular at ~17.05 and ~20.20 2 θ degrees, which were weak in intensity, and which can be assigned to the dihydrate form. The PXRD pattern of this sample may be described as a combination of the mono and dihydrate forms.

Between 60 and 70% RH the sample adsorbed nearly 6% of water relative to the initial mass of monohydrate. PXRD of the recovered and analysed material (Fig. 4 d) indicated the presence of a dihydrate, with the peak pattern corresponding with the material which was subjected to single crystal analysis (section 3.2) (Fig. 2 a). Overall TGA mass loss in the range from 25-200°C was ~12%, divided into two steps of 7.4% and 4.9% (Fig. 5. 2 e), corresponding with respective onsets of peaks on the DSC at 57.0°C and 157.8°C, due to the first and second stages of water evaporation (Fig. 5. 1 e). Further conditioning of CTZK dihydrate form II, at 80 and 90% RH did not result in additional changes (Fig. 4 c) to the PXRD pattern, nor to DSC and TGA profiles of the dihydrated material (Fig. 5. 1 d and 5. 2 d). Comparison of water vapour intake by CTZK form II to that of CTZNa dihydrate suggests that the former is less hygroscopic than the latter at high humidities (70-90% RH).

After equilibration at 90% RH the sample of CTZK form II (dihydrate) was subjected to desorption. As shown in figure 3, the sample in the range from 90 to 10% RH lost just 1.6% mass relative to the starting mass. The pattern of mass loss of CTZK dihydrate on desorption shows two different stages of approximately linear mass loss: the first in the range from 90 to 70% RH where the

mass loss was ~1%, and the second in the range from 70% to 10% RH where the sample lost a further 0.6% of water, relative to the starting mass of the monohydrate, ending up at 6.8% total water uptake. We hypothesise that the water loss in the first range (90%-70% RH) is related to adsorbed surface moisture, the second mass loss (70%-10% RH) is related to the loss of what we have described as interstitial water in form II, however it is difficult to distinguish between surface-adsorbed and interstitially captured water.

Supporting analyses by PXRD, DSC and TGA confirmed that the sample equilibrated at 10% RH remained as a dihydrate. The PXRD pattern (Fig. 4 b) remained consistent with materials equilibrated at 70% and 90% RH respectively (Fig. 4 c, d) and with raw material of form II (Fig. 4 a). DSC and TGA scans are the same for all three materials conditioned at 70%, 90% and 10% RH (after desorption) (Fig. 5. 1 c-e and 5. 2 c-e).

Below 10% RH on the desorption curve (Fig. 3), the dihydrated form collapsed and transformed to the monohydrate (form I). The change was verified by PXRD analysis (Fig. 4 f, g) and the Bragg peaks pattern was consistent with the PXRD analysis of the monohydrated raw material, form I (Fig. 2 b). DSC analysis showed a significant reduction in the size of the starting endothermal peak (Fig. 5. 1b). TGA analysis recorded mass loss in two steps. The first detectable mass loss of 1.5% may be attributed to loss of surface moisture, and the second, of 5.2%, to dehydration of the monohydrate form (Fig. 5. 2 b).

FTIR patterns of CTZK recrystallised from water and from acetone/water 1:1 mixture are similar to each other and represent the FTIR pattern of form I (Fig. 6). The bands of $-\text{CH}_3$ and $-\text{CH}_2$ groups were clearly visible in the range of 3000 cm^{-1} to 2700 cm^{-1} of CTZK form IV in contrast to the other forms of CTZK. A sharp OH stretching peak (crystallisation, bound water) was seen at around 3600 cm^{-1} for all the hydrated forms. Closer analysis of the water band revealed that this peak appeared at 3618 cm^{-1} for form I, 3595 cm^{-1} for form II and 3623 cm^{-1} for form IV indicating that this solvent was bonded most strongly in the dihydrate and most weakly in the ethanol-containing compound. A small, but clearly visible band at 3559 cm^{-1} was also noted for form II. The anhydrous form did not display the

water band, but broadening of the peaks was seen, consistent with a decreased crystallinity of this form which was supported by the pXRD pattern shown above (Fig. 2 d). The N-H stretching vibrations for this form appeared at 3357 and 3243 cm^{-1} . One of the N-H bands displayed a relatively steady position for all the three solvated forms.

It appeared at 3171, 3169 and 3191 cm^{-1} and for form I, II and IV, respectively. The other N-H peak was observed at 3354, 3428 (with a further vibration at 3359 cm^{-1}) and 3420 cm^{-1} for form I, II and IV, respectively showing greater shifts in peak positions, most likely depending on the bound solvent. This N-H peak was therefore ascribed as the N-H fragment attached to the benzene ring as it is the only N-H group in the structure directly interacting with the solvent. FTIR spectrum of form IV also differed from the di- and mono-hydrates by the presence of an extra band at 1057 cm^{-1} due to the O-CH₂ stretch vibrations from ethanol. Other characteristic bands include NH₂ deformation at 1636 cm^{-1} , asymmetric S=O stretching at 1354 cm^{-1} , symmetric S=O stretching at 1147 cm^{-1} aromatic C-H ring deformations at 1080 cm^{-1} and a bending peak associated with the NH₂SO₂ group at 961 cm^{-1} (peak positions for Form D).

The aqueous solubility of CTZK form II (dihydrate) was determined. This form was chosen due to the greatest expected stability in solution. The solubility was determined to be 78.71 ± 1.82 mg/ml (pH 8.5 ± 0.1) indicating that CTZK has an aqueous solubility ~400-fold higher compared to 0.2 mg/ml for CTZ reported previously by Charnicki and co-workers (1959).

Both, form II and IV, pseudopolymorphic structures of CTZK tend to crystallise as colourless and transparent prismatic agglomerates (Fig. 7).

3.2. Crystal structure

Single crystal X-ray analysis resulted in the determination of the molecular structures of CTZK forms II and IV. Experimental data images are reported in Fig. 8.

Chlorothiazide potassium dihydrate, form II, can be classified as an intermolecular coordinate consisting of chlorothiazide molecules bonded together with potassium. Single crystal X-ray diffraction studies (Fig. 9a) show that the structure obtained can be described as follows: $(\text{CTZ})_3 \cdot \text{K} \cdot (\text{H}_2\text{O})_2 (\text{CTZ})_2 \cdot (\text{H}_2\text{O})_2 \cdot \text{K} \cdot (\text{CTZ})_3$ (CTZK form II). The structure is of a supramolecular self-assembly type formed by several molecules of CTZ.

CTZK form II intermolecular self-assembly consists of two cations of potassium bridged by the oxygens of the sulphonyl group (O1 and O2) attached to the phenyl groups of CTZ (Fig. 9a). The bond length between the potassium and each of the oxygens is similar and is 2.67 Å and 2.75 Å for K1-O1 and K1-O2, respectively. Each of the potassium cations coordinates five molecules of chlorothiazide, four of them through the oxygens of the sulphonyl groups (O1, O2, O3 and O4) and one through the chlorine atom (Cl1). Two of the coordinated chlorothiazide molecules are bridged to the potassium through the oxygen atoms of the SO₂ group (O3 and O4) attached to the heterocyclic ring of CTZ. The bond distances between oxygen and potassium are: 2.71 Å for K1-O4 and 2.79 Å for K1-O3. The unique feature of molecular coordination observed in CTZK form II is that the potassium cation is able to coordinate the chlorine atom (Cl1-K1 distance of 3.33 Å). The distance between a chlorine atom and a potassium cation of 3.33 Å determined here is not unusual. Ellison and Levy (1964) stated for potassium hydrogen chloromaleate that: “three of the four oxygen atoms and the chlorine atom have potassium ion neighbours at significant contact distances”. The distance between the chlorine and potassium in their structure was 3.583(3). Sporer et al. (2005) reported that in K⁺(18-Crown-6) salt of triphenylmethide each potassium cation coordinated up to four chlorine atoms of the aromatic groups with average potassium–chlorine distances of 3.51–3.73 Å.

Unfortunately, information on the interatomic distances between a chlorine atom and a potassium cation is scarce as such contacts are unusual, but it appears that the distances determined in this work and referred to as “coordination” bonds fall within the values reported earlier.

To our knowledge, no reports of K-Cl coordination in salts of APIs have been published to date. Apart from interacting with CTZ, each of the potassium cations coordinates two molecules of water with the K1-O5 and K1-O6 distances of 2.86 Å and 2.65 Å, respectively. None of these water molecules is shared and/or bridged between the two cations of potassium. Additionally, a molecule of water, appearing as an interstitial/channel type, is also present in the neighbourhood of two of the potassium cations in CTZK form II. The oxygen of water is present at an equal distance of 5.39 Å from each of potassium atoms (K1-O7-K1) in the assembly. A summary of the key crystallographic information is given in supplementary data file (Table 1).

CTZK recrystallised from ethanol (form IV) presents a different crystal structure compared to CTZK form II (Fig. 9b). In CTZK form IV the two potassium cations are bridged by two oxygens of water and additionally by the oxygens of the sulphonyl group (O1, O2, O5 and O6) attached to the phenyls of two molecules of chlorothiazide (Fig. 9b). The distances between the oxygens of water (O9 and O10) and the potassium cations are 2.74 Å and 2.85 Å for K1-O9 and K1-O10, respectively and 2.88 Å and 2.71 Å for K2-O9 and K2-O10, respectively. The distances between the potassium cation and CTZ oxygens are of a similar range as those between K1/K2 and O9/O10 and are 2.80 Å and 2.76 Å for K1-O2 and K1-O6, respectively and 2.77 Å and 2.80 Å for K2-O1 and K2-O5, respectively.

CTZK form IV is composed of two types of CTZ molecules that are crystallographically independent (Fig. 8). The two potassium cations in CTZK form IV coordinate a different number of atoms each. They both coordinate six oxygens, but one of them additionally coordinates one chlorine atom of CTZ (Cl2-K2) with a distance of 3.57 Å. The distance between the potassium and chlorine in CTZK form II described above was shorter i.e. was 3.33 Å. In CTZK form IV one of potassium ions (K1) coordinates four molecules of chlorothiazide through oxygens of the sulphonyl groups: two from the phenyl ring mentioned before (O6, O4 shared with the second potassium cation) plus two from the

heterocyclic ring of chlorothiazide (O2 and O1). The distances between the potassium atom and oxygens of the sulphonyl group of the heterocyclic ring of CTZ are: K1-O3: 2.75 Å and K1-O4: 2.71 Å. The other potassium (K2) coordinates five molecules of chlorothiazide: four of them are coordinated by the oxygens of the sulphonyl group: three from the benzene ring (O3, O5 and O7) plus the fourth oxygen of the heterocyclic ring (O30). The fifth chlorothiazide molecule is coordinated to the potassium ion through the chlorine atom of the CTZ molecule.

Extensive network of hydrogen bonds were determined in both of the pseudopolymorphic forms (II and IV) of CTZK and are presented in Table 1.

CTZK from IV occurs as a monohydrate additionally containing molecules of ethanol with the molar ratio of H₂O: ethanol: CTZ of 2:1:2 based on the single crystal X-ray analysis, in excellent agreement with the ratio determined by thermal analysis and GC-MS (section 3.1). It has a different crystal unit cell than CTZK form II (Supplementary data file Table 1). While CTZK form II is monoclinic with a space group of C2/c, CTZK form IV has a triclinic crystal structure and a space group of P-1.

To date only a limited number of APIs containing similar coordinates formed by potassium cation have been described and reported, suggesting that crystal structures of pharmaceutically relevant potassium salts have not been widely investigated. Geddes et al. (1974) reported a crystal structure of nigericin potassium salt and compared it with a nigericin silver salt. In nigericin, the potassium cation coordinates seven oxygen atoms with distances between the oxygens and potassium between 2.58 Å and 3.09 Å. All the coordinated oxygens come from the same molecule of nigericin i.e. the structure of the complex is 1 molecule of K⁺ to 1 molecule of nigericin. On the other hand, Tauvel et al. (2009) described crystal structures of a potassium salt of tenatoprazole. Depending on the solvent used, the mono-potassium salt of tenatoprazole presented the following forms: a monoclinic- diethanolate, a monoclinic-(x)methanolate,-(2-x)ethanolate, where (0≤x<1), diethanolate and an orthorhombic structure of ethylenglycolate (EG). Similarly to CTZK, a hydrated form of potassium tenatoprazole recrystallised from ethanol. The authors observed 1D ribbon arrangements for the diethanolate and ethylenglycolate

forms of the API, therefore showing that a supramolecular organisation for potassium salts is possible, however CTZK (especially form IV) exhibits a complex crystal structure compared to those previously described.

Bekdemir et al. (2002) published the crystal structure of potassium p-nitrobenzoxasulfamate monohydrate. This orthorhombic structure is based on two cations of potassium which, as in the CTZK form III structure, are crystallographically independent. One of the potassium cations coordinated six oxygens in the range 2.6538-3.0916 Å and one atom of nitrogen (2.9236 Å) while the second potassium cation coordinated seven atoms of oxygens in the range 2.7502-3.0468 Å and one nitrogen (2.7942 Å).

^1H NMR and ^{13}C NMR analyses of CTZK form II and IV confirmed the chemical structure of the API molecule, supporting the single crystal X-ray diffraction results. The primary amine group of CTZ was found to be deprotonated, as reported for CTZNa (Paluch et al, 2010). The full NMR characterisation of CTZK form II and IV can be found in Supplementary Content.

3.3. Hirshfeld surfaces

Hirshfeld surfaces analysis allowed for visualisation and comparison of reciprocal interactions among atoms in crystal lattices of CTZK form II and form IV. The visualisation is based on a 3-D surface surrounding a single molecule of CTZK. Parameters describing this surface are d_i and d_e , where d_i corresponds to the distance between the surface and atom placed the closest internally to the surface. d_e corresponds to the distance between the surface and atom placed the closest externally to the surface. Presented surfaces by d_{norm} are the sum of d_i and d_e where each of them is normalised to the van der Waals radius of the involved atom. 3-D images of surfaces of molecules are partially coloured and partially gray. The colour spectrum ranges from blue to white to red. If the surface is coloured blue, it means, that reciprocal interactions between two molecules placed internally and externally to the Hirshfeld surface are longer (weaker) on a relative scale than van der Waals forces. White planes are equal to van der Waals distance, while red surfaces represent interactions stronger than van der Waals

forces. The surfaces presented in Fig. 10 reveal the close contacts between the atoms highlighting hydrogen bond donors and acceptors and interactions of the potassium ions.

The 3-D surface (Fig. 10) surrounding the molecule can be depicted by a D-2 fingerprint plot (Fig. 11) where $d_e=f(d_i)$. The fingerprint plot is pseudo-mirrored along $d_e=d_i$ which reflects the reciprocated interactions between selected atoms. The fingerprint plot depicts the percentage of overall Hirshfeld surface covered by a particular type of bond. This is important as red strong interactions, so called hot-spots, can be crucial in the formation of a particular crystal structure, but will not cover a large percentage of the Hirshfeld surface, so the overall stabilising effect on the crystal structure can be weaker than the less intensive blue interaction, but which covers a larger percentage of the Hirshfeld surface.

Figures 11 and 12 illustrate decomposition of the fingerprint plots for CTZ II and IV. This detailed analysis allows one to discern that the largest contribution to the overall Hirshfeld surface in CTZK form II are O...H, O...O and O...K (Fig. 11) and in form III are H...H, O...H and O...O (Fig. 12) contacts, suggesting that weak but repulsive H...H contacts contribute to the stability of CTZK form IV.

Both fingerprints presented the appearance of spikes characteristic of hydrogen bonds involving O...H and N...H contacts. The fingerprint plot of CTZK form II is quite asymmetric and this asymmetry is due to the presence of the channel water molecule. The fingerprint plots can also be considered in terms of hydrogen bond donors/acceptors, where $d_e>d_i$ contacts correspond to the hydrogen bond donors and $d_e<d_i$ contacts indicate the hydrogen bond acceptors. This examination indicates that the O...H contacts are more sensitive to the inclusion or exclusion of the solvated water molecules compared to contacts of other types. The hydrated CTZK form II, inclusive of the channel and coordinated by the K^+ water molecules, has 17.1% O...H (H-bond acceptors), 11.3% H...O (H-bond donors) as well as 5.4% O...K, 7.1% K...O and 16.7% O...O contacts contributing towards stability of the crystal structure of this form. Exclusion of the channel water only slightly changed these proportions to: 16.0% O...H, 9.6% H...O, 5.6% O...K, 7.7% K...O and 14.6% O...O interactions.

Removal of all water molecules hydrating the CTZK altered the contributions of H...O and H...O contacts to 9.9% and 12.9%, respectively and changed the balance of H-bond donors and acceptors able to interact with the groups participating in such contacts. This suggests that the water molecules bound by the potassium ions are essential for maintaining of the crystal lattice integrity of form II, whereas exclusion of the channel water impacts on the stability to a much lesser degree. The proportions of the O...K, K...O and O...O contacts in the fully water deprived structure are 5.9%, 12.7% and 9.6%, respectively.

In form IV, the mixed ethanolate/hydrate form, the O...H/H...O contributions change as follows: 10.9%/8.9%, 15.5%/5.8%, 9.1%/9.0% and 13.5%/6.5% for the fully solvated form IV, the structure with ethanol excluded but water molecules left in, the structure with water excluded but ethanol left in and the desolvated form (water and ethanol excluded), respectively. This, in contrast to form II, indicates that both of the solvents may be important in maintaining the integrity of form IV. Omission of water of solvation results in a change of the O...K and K...O contacts from approximately 5% and 6% to approximately 4% and 9%, respectively, not surprisingly as the water interacts with the potassium ions directly. Form II and form IV also display a significant difference in the contribution of H...H weak contacts, 5.2% and 24.2%, respectively showing a greater contribution of these weak interactions arising from interaction of hydrogen atoms of the ethanol molecules with adjacent aromatic rings of CTZK.

4. Conclusions:

Chlorothiazide formed a range of intermolecular self-assemblies (ISA) with potassium cations when crystallised from different liquid environment by solvent evaporation.

Potassium cations of CTZK can coordinate up to seven atoms (oxygens of water, oxygens of sulphonyl groups and the chlorine of CTZ molecule). The potassium cations are not bridged by water in CTZK recrystallised from water, whereas a more complex coordinate with two types of crystallographically independent CTZ molecules, is formed in CTZK ISA recrystallised from ethanol (form IV). In the latter, the potassium cations do not coordinate an equal number of atoms (K1 coordinates seven and K2 coordinates six). Potassium cations deprotonate the primary amine groups of CTZ and shift the proton of the secondary amine group in the heterocyclic ring of CTZ, analogous to results reported for CTZNa (Paluch et al. 2010).

The different CTZK forms have different physical stabilities when temperature and/or humidity is changed. Drying form IV leads to evaporation of ethanol present in the crystal lattice, but not water, and transforms the original crystals to a desolvated material (CTZK form V) that has a different Bragg peak pattern compared to CTZK form I (monohydrate). The latter can be obtained by crystallisation from water but is also found to form by direct drying of CTZK form II. DVS analysis showed that CTZK form I had better moisture-related stability than CTZNa monohydrate and was stable up to 60% RH (at 25 °C). The dihydrate (form II) existed over a broad range of relative humidities, 10-90%RH, at 25°C. Extensive drying of form I results in an anhydrous material (form III) which was seen to be exceptionally moisture sensitive and converted to form I even at a very low humidity of 0.5-0.7% RH in the DVS at 25°C. This contrasted with the behaviour of CTZNa anhydrous form which was stable up to 20% RH (Paluch et al., 2010). The rich solvatomorphism of CTZK presented here is in contrast to some reports that the potassium cation forms hydrated salts less readily than the sodium cation (Remington, 2005). However, the solvates of CTZK seem to be less hygroscopic compared with the hydrated CTZNa, consistent with previously published data (Swarbrick, 2007).

The aqueous solubility of CTZK dihydrate was estimated to be 78.71 ± 1.82 mg/ml, 400-fold higher than that of CTZ (Charnicki et al. 1959), thus indicating a biopharmaceutical advantage for the salt form.

Accepted Manuscript

Acknowledgements

The authors wish to acknowledge funding for this research from the Irish Research Council for Science and Engineering Technology (IRCSET) and the Solid State Pharmaceutical Cluster (SSPC), supported by Science Foundation Ireland under grant number [07/SRC/B1158].

Authors would like to thank Professor Brian McMurry for scientific consultation of single crystal data and Mr. Adam Coburn University College Dublin, Department of Chemistry, for elemental analysis.

Accepted Manuscript

References:

- Adams, M.E., Subhash, D., Aziz, K., Kalidas, P., Douglas, J.S., Zold, D.J., 2000. Potassium, sodium and tris oxaprozin salt pharmaceutical formulations, US Patent 6030643.
- Antoncic, L., Copar, A., 2009. Preparation of telmisartan salts with improved solubility. US Patent Application: 20090012140.
- Appel, L.J., 2002. The verdict from ALLHAT-thiazide diuretics are the preferred initial therapy for hypertension. *JAMA*, 18, 3039-3042.
- Bekdemir, Y., Kutuk, H., Celik, S., Yilmaz, V.T., Thoene, C., 2002. Trans-Tetraaquabis (p-nitrobenzoxasulfamato)cobalt(II), *J. Mol. Struct.*, 604, 239-244.
- Blagden, N., de Matas, M.P.T., York, G.P., 2007, Crystal engineering of active pharmaceutical ingredients to improve solubility and dissolution rates, *Adv. Drug Deliv. Rev.* 59, 617-630.
- Blessing, R.H., 1995. An empirical correction for absorption anisotropy. *Acta Cryst.* A51, 33-38.
- Brunton, L.L., Lazo, J.S., Parker, K.L., (Eds.), 1996. Goodman and Gilman's The Pharmacological Basis of Therapeutics. The McGraw-Hill, New York.
- Charnicki, W.F., Bacher, F.A., Freeman, S.A., Decesare, D.H., 1959. The pharmacy of chlorothiazide (6-chloro-7-sulfamyl-1,2,4-benzothiadiazine-1,1-dioxide) - a new orally effective diuretic agent. *J. Am. Pharm. Assoc.* 48, 656-659.
- Derry, P., Derry, S., Moore, R.A., McQuay, H.J., 2009. Single dose oral diclofenac for acute postoperative pain in adults, *Cochrane Database Syst. Rev.*, 2, CD004768.
- Ellison, D.H., Loffing, J., 2009. Thiazide effect and adverse effects: Insights from molecular genetics. *Hypertension*, 54, 196-202.
- Ellison, R.D., Levy, H., A., 1965, A Centered Hydrogen Bond in Potassium Hydrogen Chloromaleate: A Neutron Diffraction Structure Determination, *Acta Cryst.*, 19, 260- 268.
- European Pharmacopoeia. 6th ed., 2007. Council of Europe, Strasbourg.

- Farrugia, L.J., 1997. ORTEP-3 for Windows - a version of ORTEP-III with a Graphical User Interface (GUI). *J. Appl. Crystallogr.* 30, 565.
- Geddes, A.J., Sheldrick, B., Stevenson, W.T.J., Steinrauf, L.K., 1974. The crystal structure of the potassium salt of nigericin, *Biochem. Biophys. Res Commun.*, 60,1245-1251.
- Healy, A.M., McDonald, B.F., Tajber, L., Corrigan, O.I., 2008. Characterisation of excipient-free nanoporous microparticles (NPMPs) of bendroflumethiazide. *Eur. J. Pharm. Biopharm.* 69, 1182-1186.
- Hirshfeld, F.L., 1977. Bonded-Atom Fragments for Describing Molecular Charge-Densities *Theor. Chim. Acta*, 44, 129-138
- Jakobsen, P., Treppendahl, S., 1979. Structure of 1,2,4-benzothiadiazine-1,1-dioxides. *Tetrahedron* 35, 2151-2153.
- McKinnon, J.J., Spackman, M.A., Mitchell, A.S., 2004. Novel tools for visualizing and exploring intermolecular interactions in molecular crystals, *Acta Cryst. B*, 60, 627-668.
- Paluch, K.J., Tajber, L., McCabe, T., O'Brien, J.E., Corrigan, O.I., Healy, A.M., 2010. Preparation and solid state characterisation of chlorothiazide sodium intermolecular self assembly suprastructure, *European Journal of Pharmaceutical Sciences*, EJPS-D-10-00480
- Remington: the science and practice of pharmacy, 2005. 21st Edition, Lippincott Williams & Wilkins.
- Scholz, E., 1987. Reagents for Karl Fischer Titration. Riedel-de Haën Aktiengesellschaft.
- Spek, A.L., 2003. Single-crystal structure validation with the program PLATON. *J. Appl. Crystallogr.* 36, 7-13.
- Sporer, C., Ratera, I., Wurst, K., Vidal-Gancedo, J., Ruiz-Molina, D., Rovira, C., Veciana, J., 2005. Ferrocene triphenylmethyl radical donor–acceptor compounds. Towards the development of multifunctional molecular switches, *ARKIVOC*, 2005, (IX), 104-114.
- Stahl, P.H., Wermuth, C.G., 2008. Handbook of pharmaceutical salts properties, selection and use, Wiley-VCH.
- Swarbrick, J., 2007. Encyclopedia of pharmaceutical technology, Informa Healthcare USA, Inc.

Tajber, L., Corrigan, D.O., Corrigan, O.I., Healy, A.M., 2009. Spray drying of budesonide, formoterol fumarate and their composites-I. Physicochemical characterisation. *Int. J. Pharm.* 367, 79-85.

Tajber, L., Corrigan, O.I., Healy, A.M., 2005. Physicochemical evaluation of PVP-thiazide diuretic interactions in co-spray-dried composites - analysis of glass transition composition relationships. *Eur. J. Pharm. Sci.* 24, 553-563.

Tauvel, G., Sanselme, M., Coste-Leconte, S., Petit, S., Coquerel, G., 2009. Structural studies of several solvated potassium salts of tenatoprazole crystallizing as conglomerates, *J. Mol. Struct.* 936, 60-66.

Wu, C.Y., Benet, L.Z., 2005. Predicting drug disposition via application of BCS: transport/absorption/elimination interplay and development of a biopharmaceutics drug disposition classification system, *Pharm. Res.*, 22, 11-23.

CCDC 761198 and 761199 contains the supplementary crystallographic data for this paper. These data can be obtained free of charge from The Cambridge Crystallographic Data Centre via www.ccdc.cam.ac.uk/data_request/cif

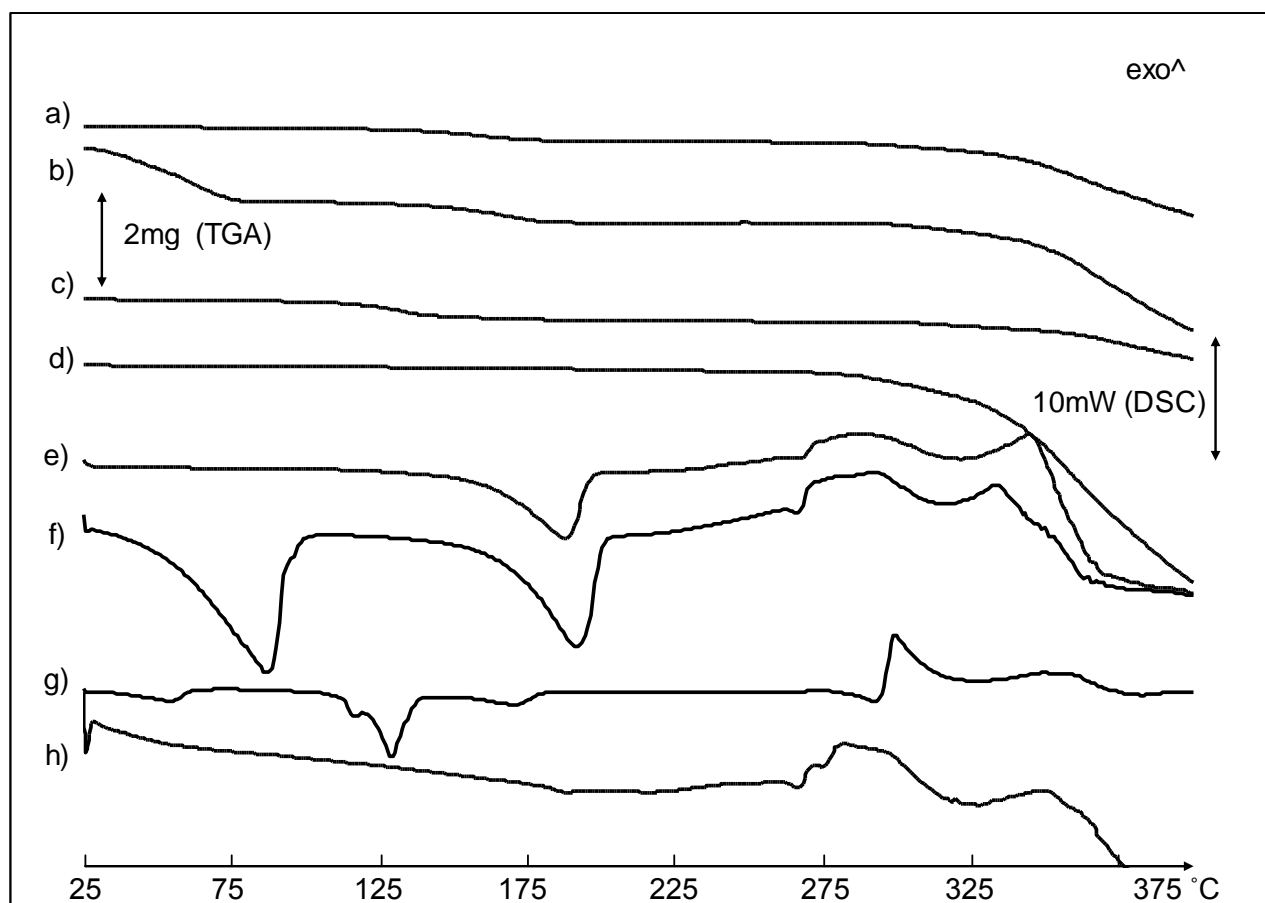


Fig. 1. Thermal analysis of CTZK: a) TGA scan of CTZK form I, b) TGA scan of CTZK form II, c) TGA scan of CTZK form IV, d) TGA scan of CTZK form III (anhydrous), e) DSC scan of CTZK form I, f) DSC scan of CTZK form II, g) DSC scan of CTZK form IV, h) DSC scan of CTZK form III (anhydrous).

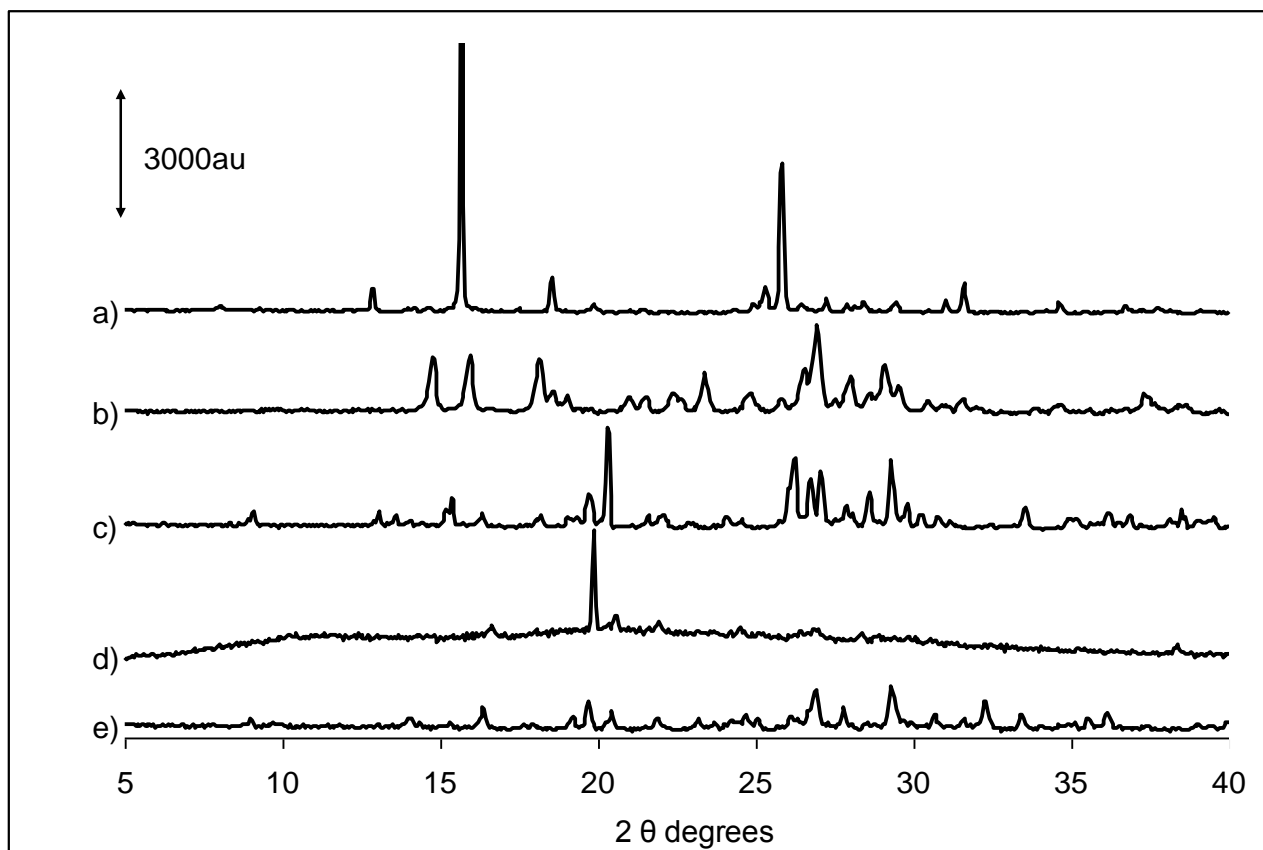


Fig. 2. PXRD pattern of CTZK: a) form IV (monohydrate hemiethanolate) , b) form I (monohydrate), c) form II (dihydrate), d) form III (anhydrous), e) form V (desolvated monohydrate hemiethanolate).

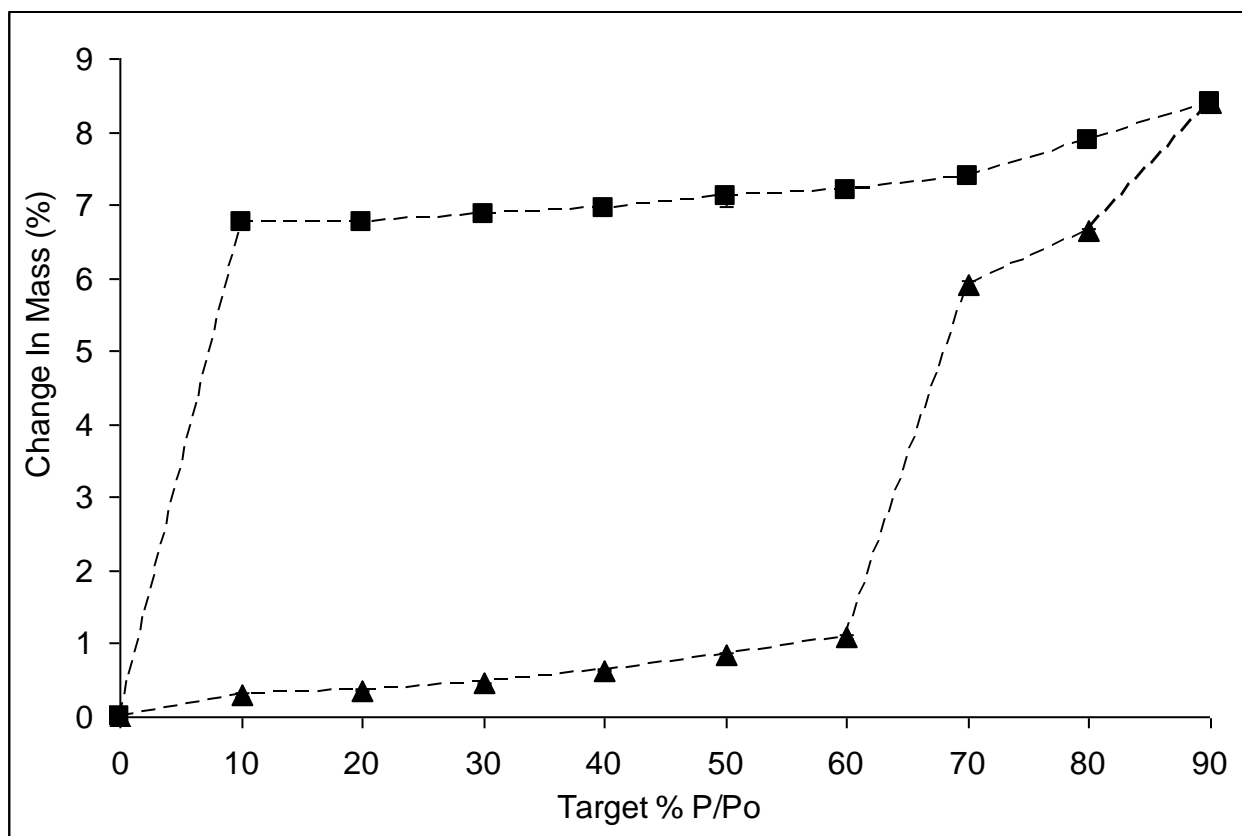


Fig. 3. Isothermal (25°C) plot of sorption (triangle) and desorption (square) of water vapour for CTZK form I (monohydrate).

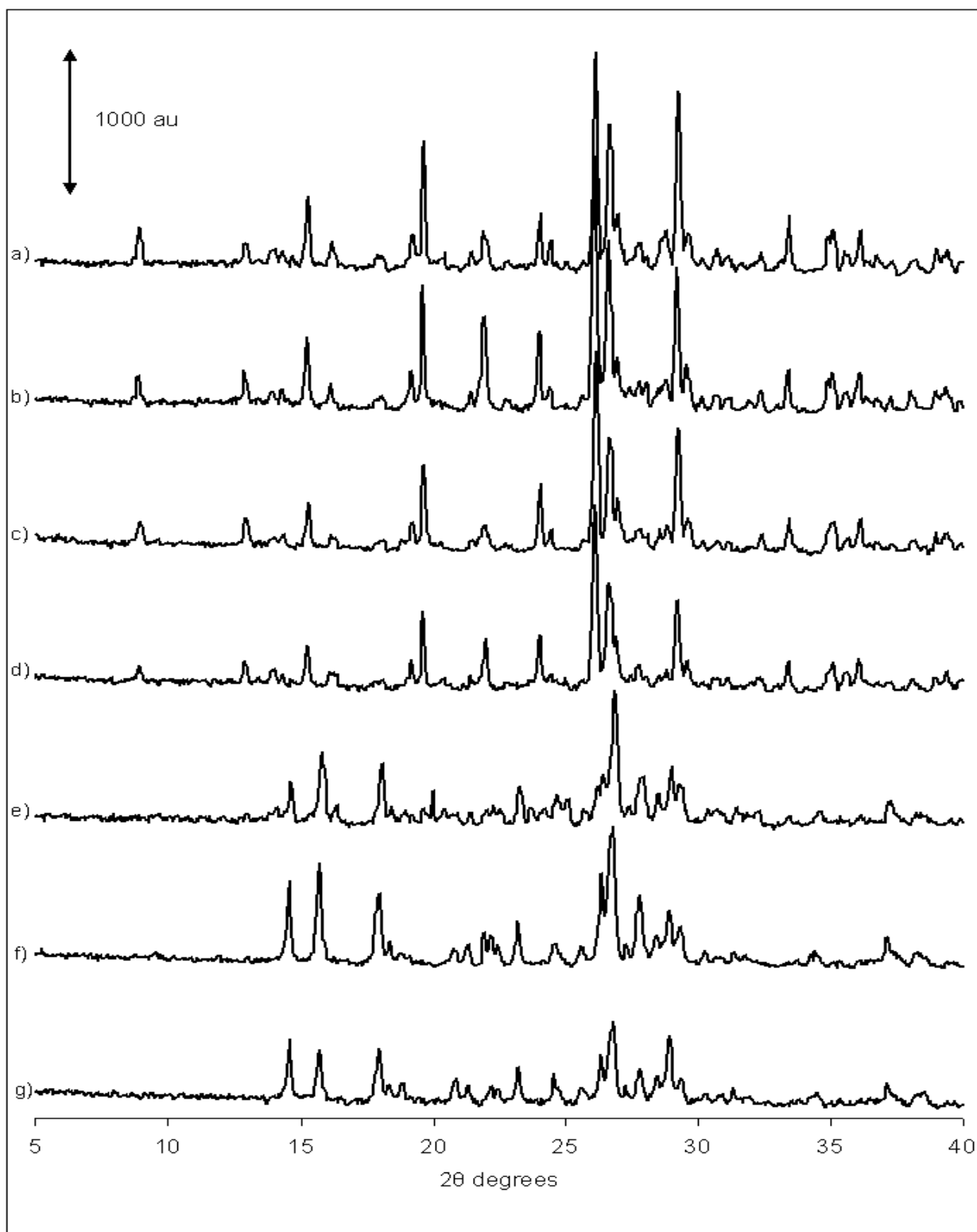
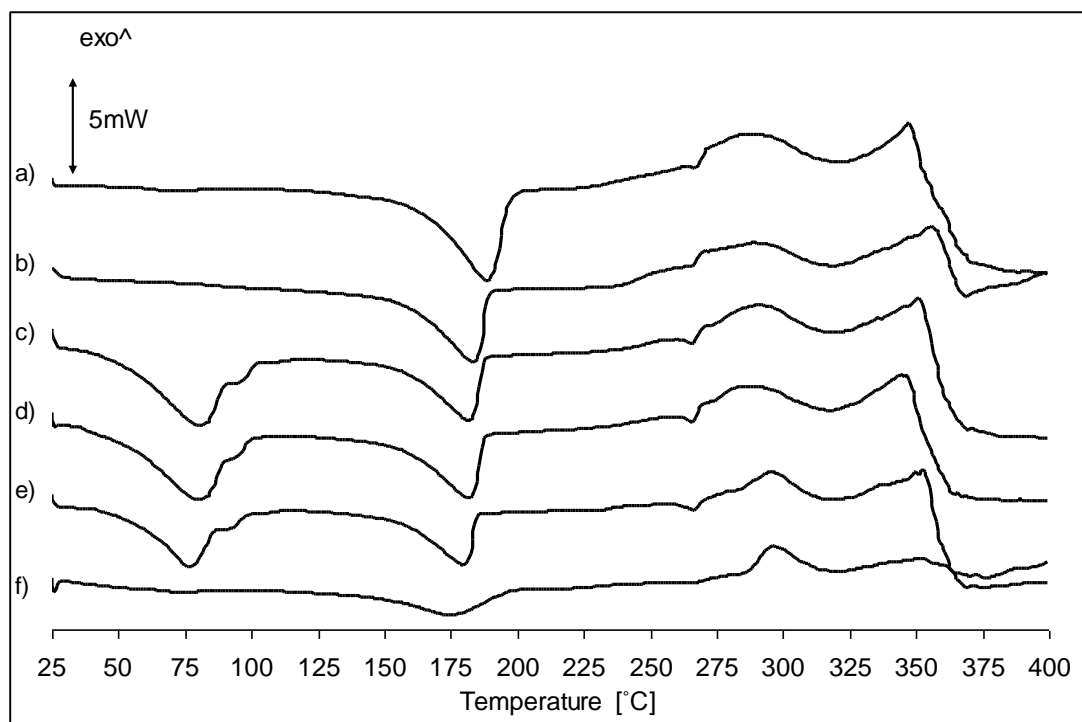
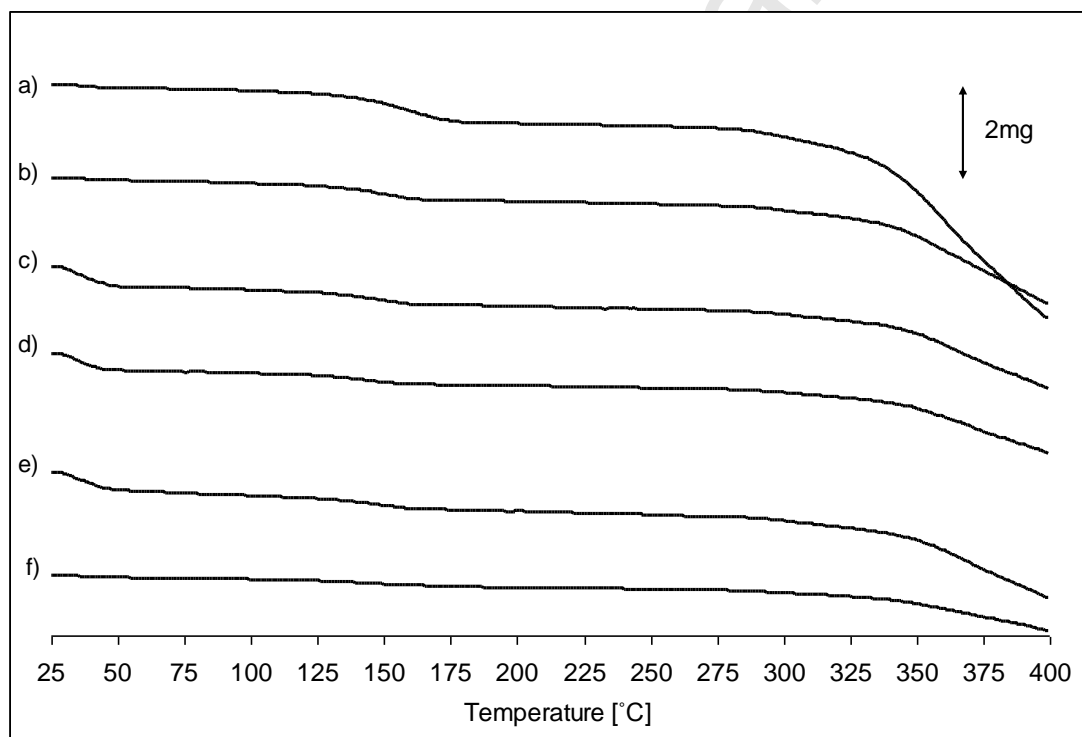


Fig 4. PXRD results of CTZK: a) dihydrate raw material, b) dihydrate, equilibrated at 10%RH, c) dihydrate equilibrated at 90%RH, d) dihydrate equilibrated at 70%RH, e) monohydrate equilibrated at 60%RH, f) monohydrate equilibrated at 0%RH (starting material: monohydrate), g) monohydrate equilibrated at 0%RH (starting material: dihydrate).



I



II

Fig. 5. DSC (I) and TGA (II) analysis of CTZK: a) monohydrate starting material equilibrated at 0% RH, b) monohydrate equilibrated at 0% RH after desorption, c) dihydrate equilibrated at 10% RH, d) dihydrate equilibrated at 90% RH, e) dihydrate equilibrated at 70% RH, f) monohydrate equilibrated at 60% RH.

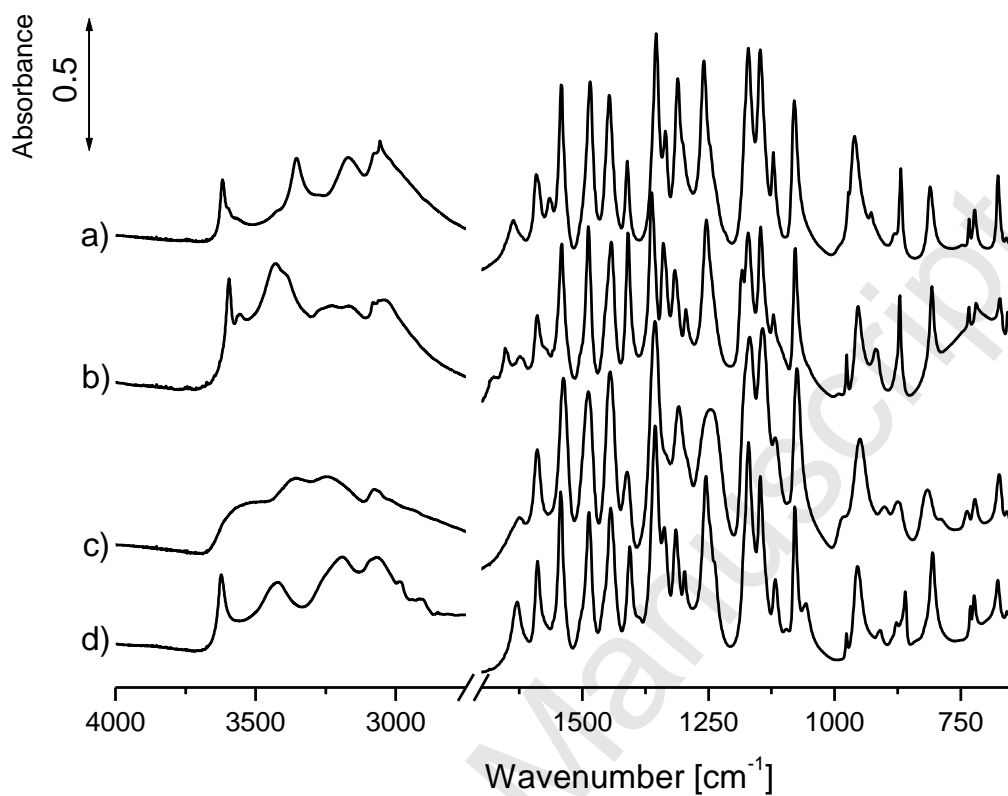
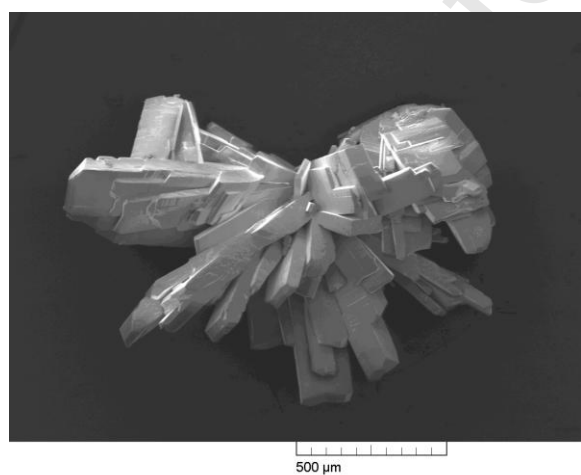
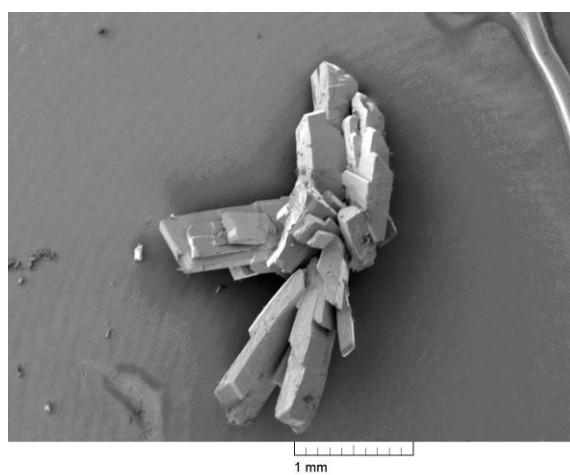


Fig. 6. FTIR analysis of CTZK: a) form I, b) form II, c) anhydrous form III, d) form IV.



a)



b)

Fig. 7. SEM images of CTZK: a) form II, b) form IV.

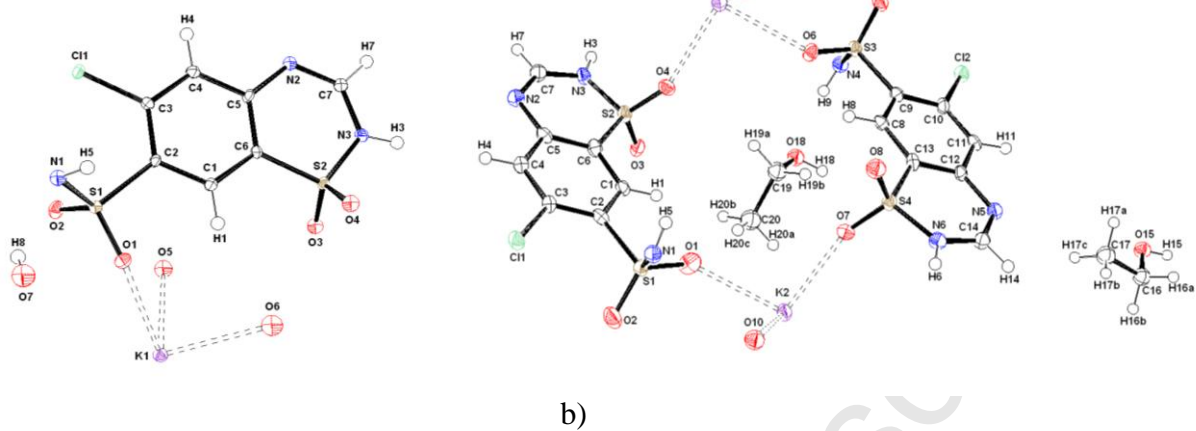


Fig. 8. View of chlorothiazide potassium: a) dihydrate (CTZK form II), b) monohydrate hemiethanolate (CTZK form IV) by Ortep visualisation.

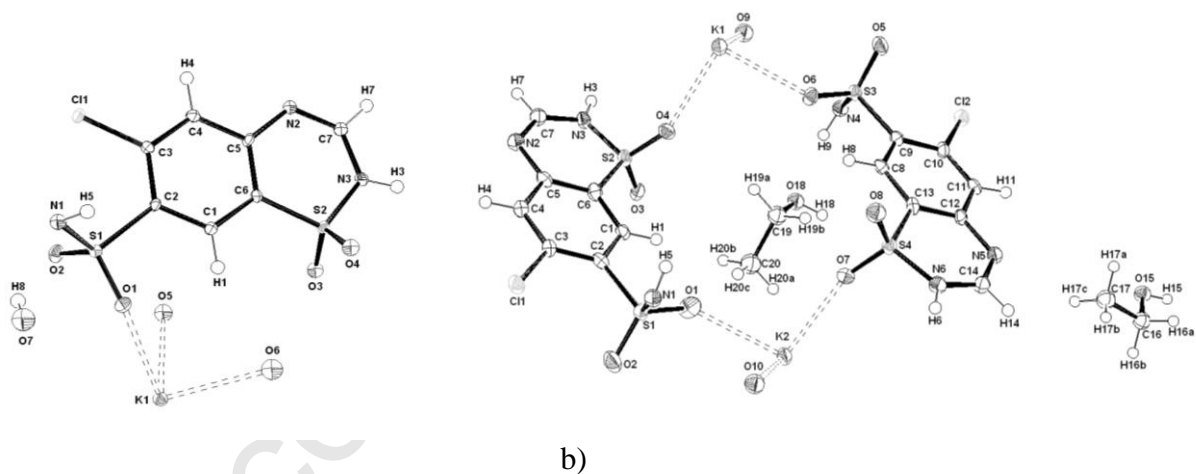
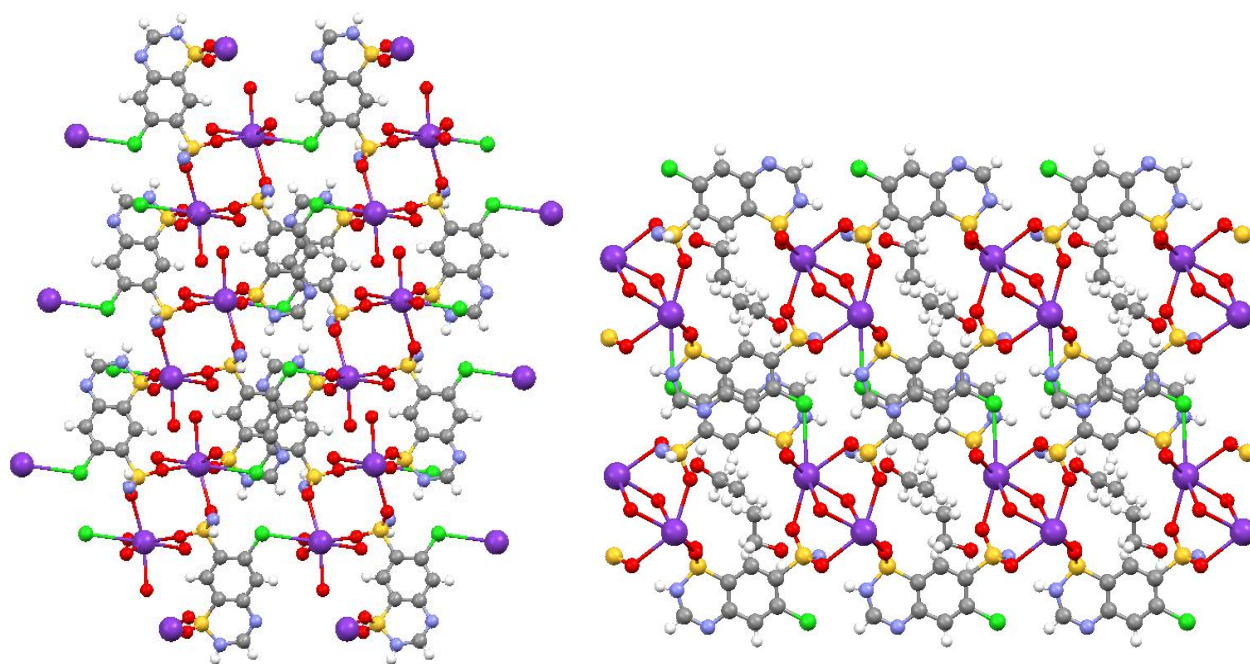


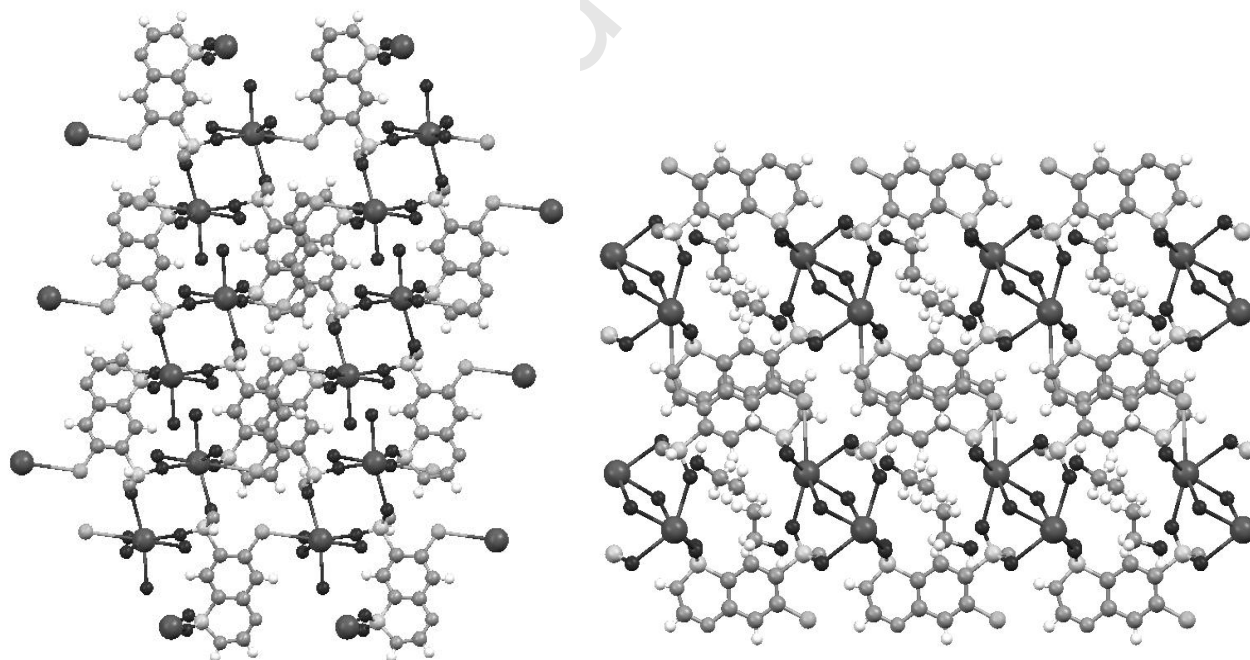
Fig. 8. View of chlorothiazide potassium: a) dihydrate (CTZK form II), b) monohydrate hemiethanolate (CTZK form IV) by Ortep visualisation.



a)

b)

Fig. 9. Crystal cell packing: a) CTZK form II view along “b” axis, b) CTZK form IV view along “a” axis,



a)

b)

Fig. 9. Crystal cell packing: a) CTZK form II view along “b” axis, b) CTZK form IV view along “a” axis,

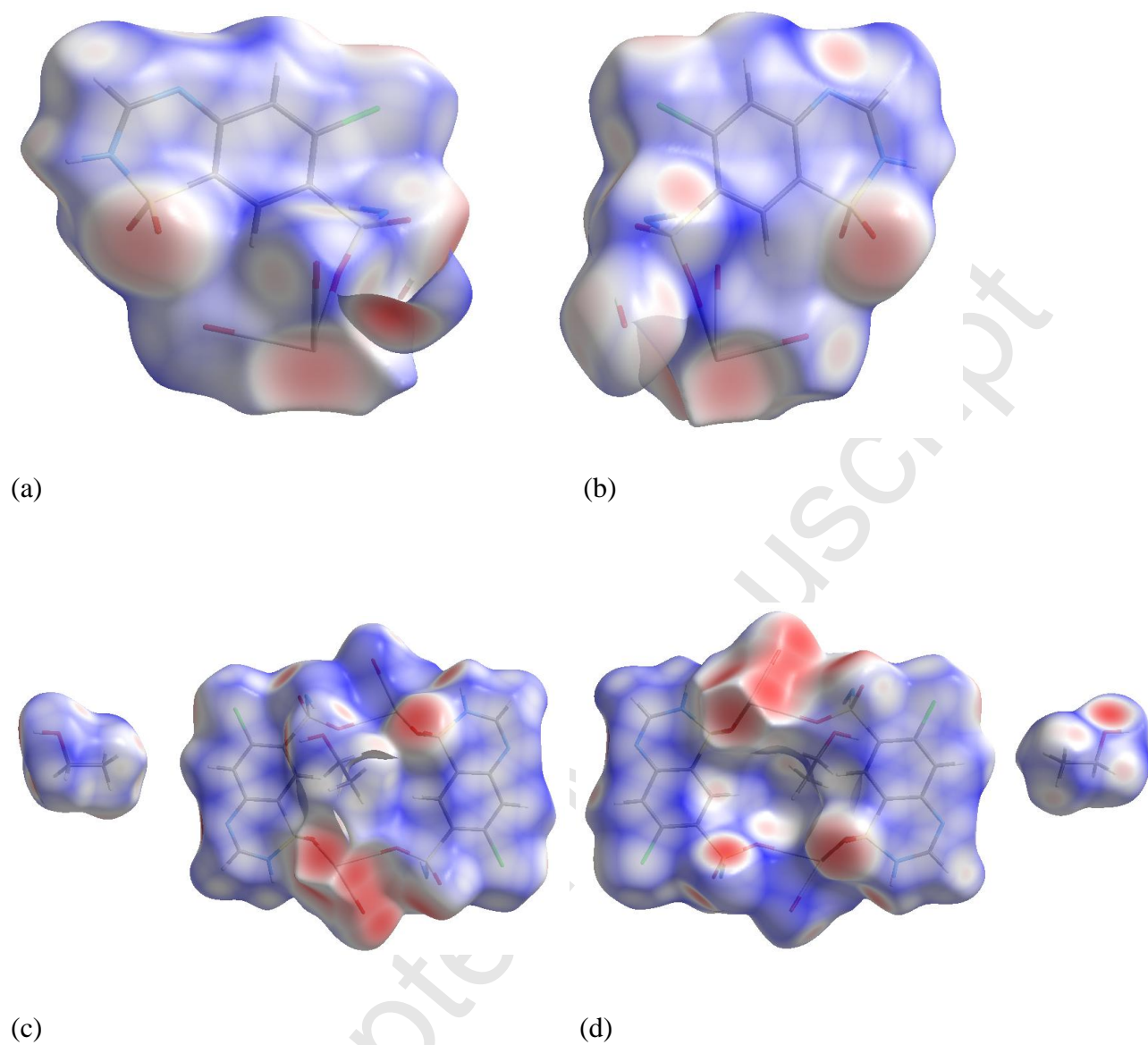


Fig. 10. (a) Front, (b) back view of d_{norm} mapped on the Hirshfeld surface of Form II, (c) front and (d) back view of d_{norm} mapped on the Hirshfeld surface of Form IV.

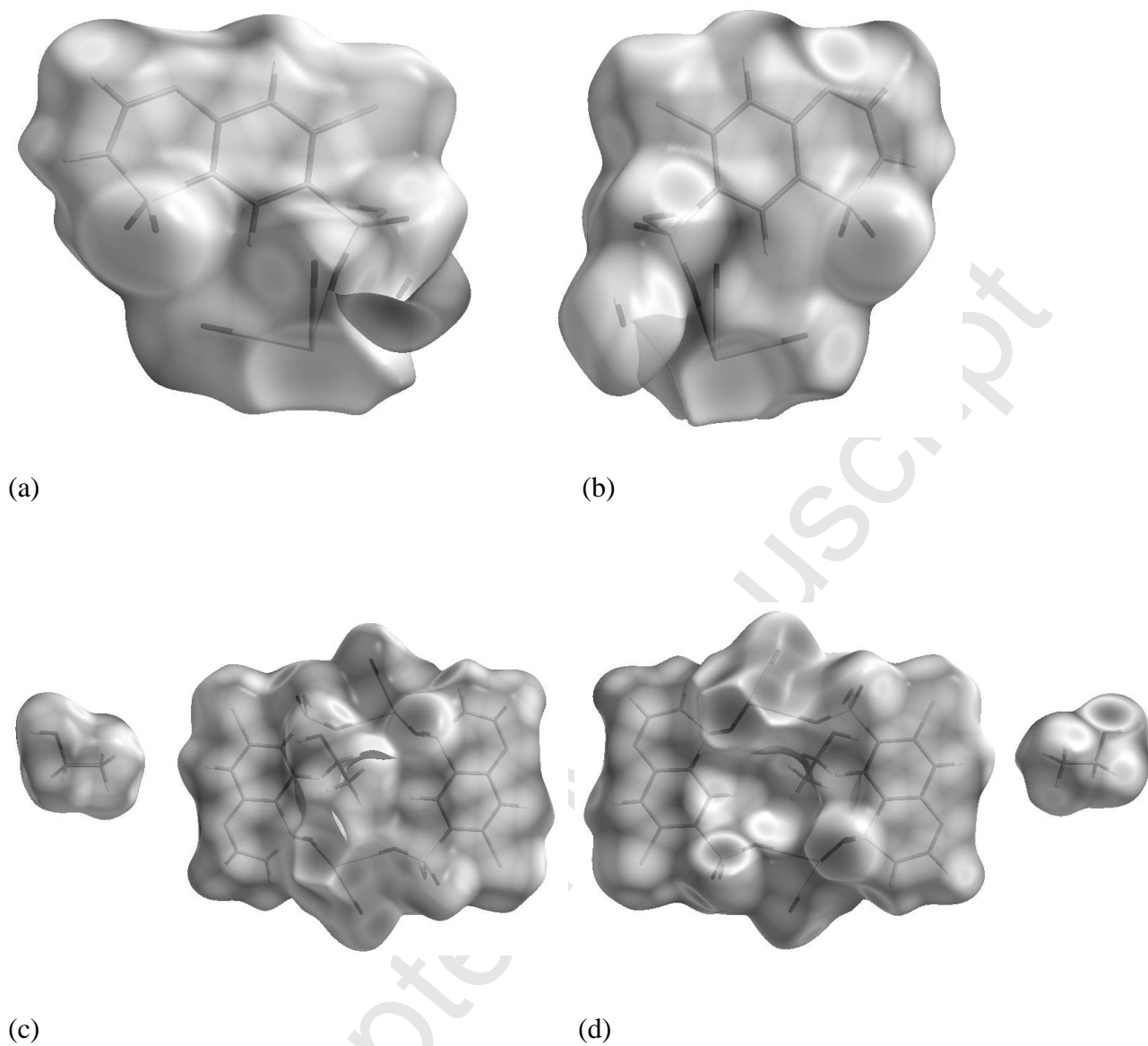


Fig. 10. (a) Front, (b) back view of d_{norm} mapped on the Hirshfeld surface of Form II, (c) front and (d) back view of d_{norm} mapped on the Hirshfeld surface of Form IV.

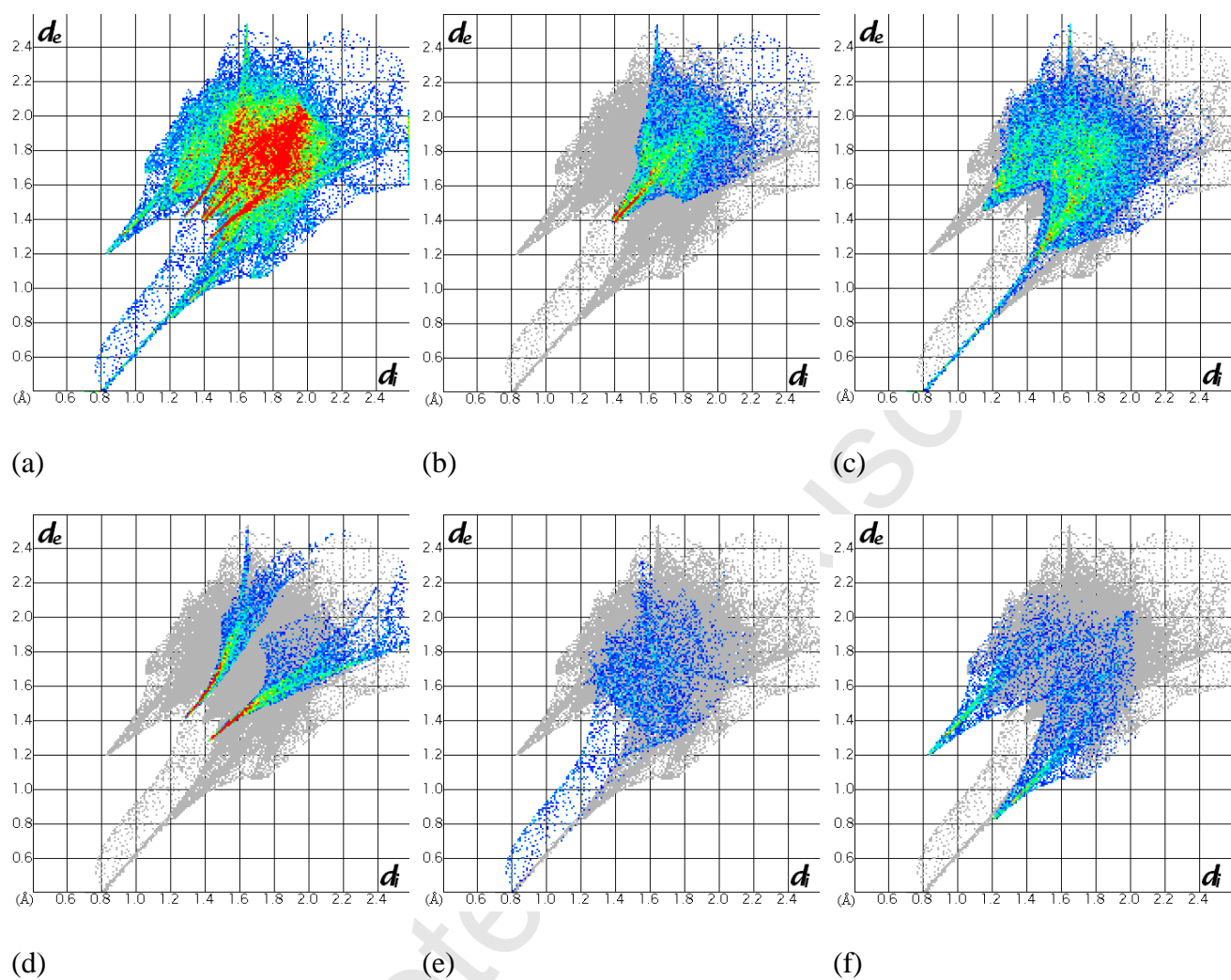


Fig. 11. Full (a) and partial fingerprint plots for CTZK form II: b) O...O contacts (16.7%), c) O...H reciprocal contacts (28.4%), d) O...K reciprocal contacts (12.5%), e) H...H contacts (5.2%), f) N...H reciprocal contacts (8.0%).

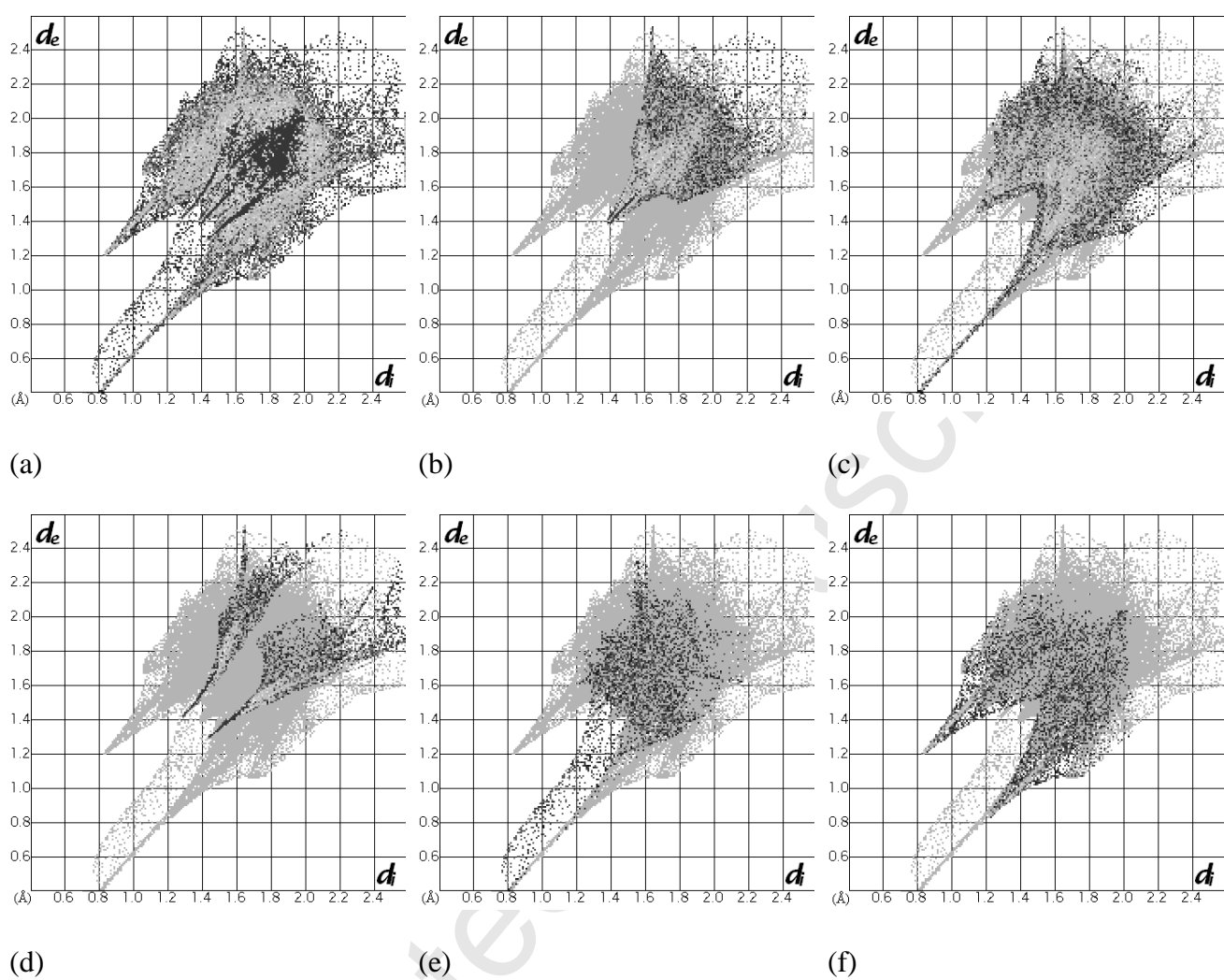


Fig. 11. Full (a) and partial fingerprint plots for CTZK form II: b) O...O contacts (16.7%), c) O...H reciprocal contacts (28.4%), d) O...K reciprocal contacts (12.5%), e) H...H contacts (5.2%), f) N...H reciprocal contacts (8.0%).

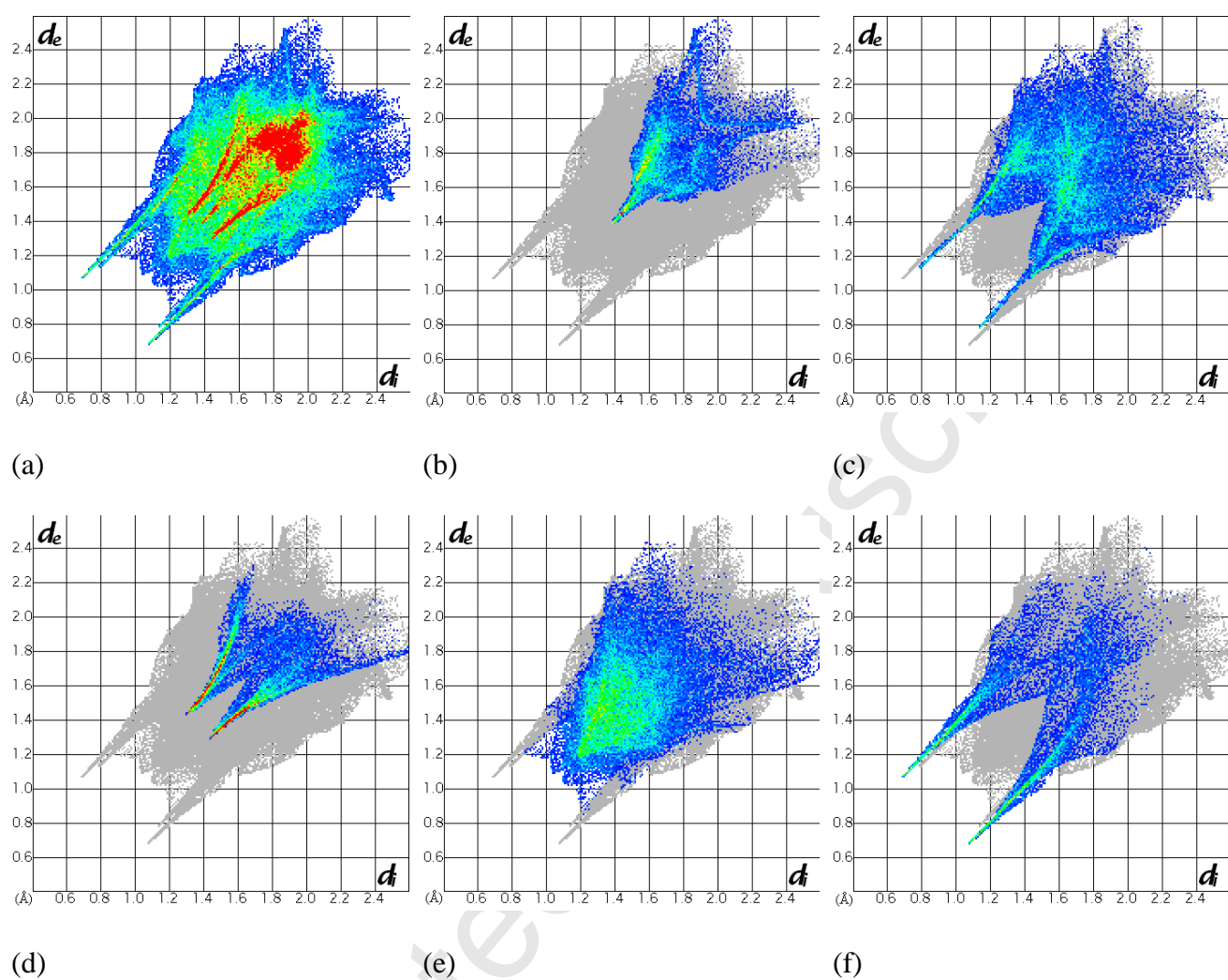


Fig. 12. Full (a) and partial fingerprint plots for CTZK form IV: b) O...O contacts (9.8%), c) O...H reciprocal contacts (19.7%), d) O...K reciprocal contacts (9.5%), e) H...H contacts (24.2%), f) N...H reciprocal contacts (8.1%).

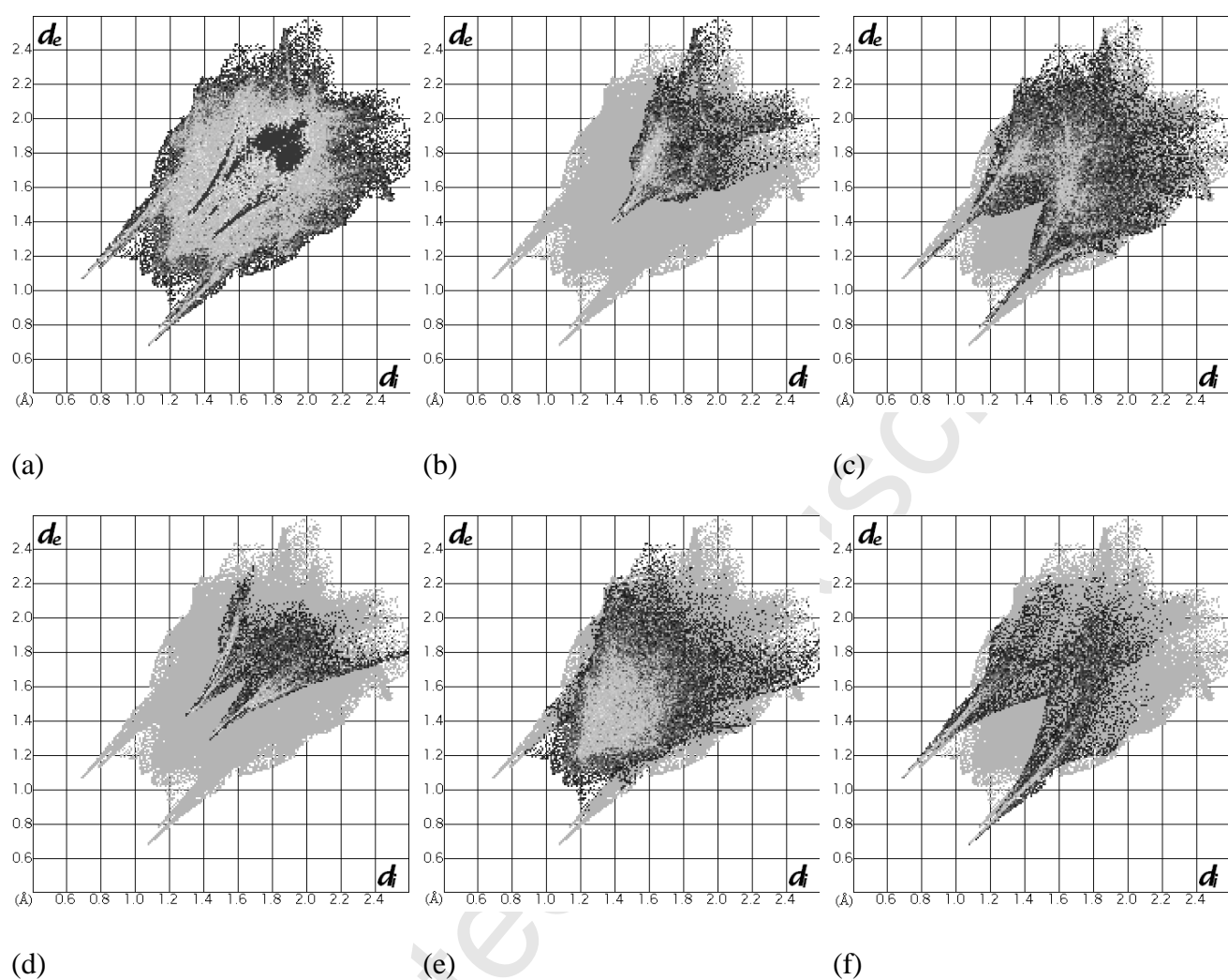


Fig. 12. Full (a) and partial fingerprint plots for CTZK form IV: b) O...O contacts (9.8%), c) O...H reciprocal contacts (19.7%), d) O...K reciprocal contacts (9.5%), e) H...H contacts (24.2%), f) N...H reciprocal contacts (8.1%).

Table 1. Bond lengths and dihedral angles for hydrogen bonding interactions in CTZK form II and CTZK form IV.

Bond type D-H...A	D-H [Å]	H...A [Å]	D...A [Å]	D-H...A [°]
CTZK form II				
N3-H3...N1 (a)	0.88	2.15	2.933(4)	148
N1-H5...N2 (b)	0.82(5)	2.38(6)	3.027(3)	136(5)
O7-H8...N1	0.97(6)	2.29(6)	3.069(3)	138(5)
C1-H1...O1	0.95	2.41	2.824(4)	106
CTZK form IV				
N3-H3...N1 (c)	0.88	2.22	2.998(5)	148
N1-H5...O15 (d)	0.83(5)	2.09(5)	2.922(5)	173(4)
N6-H6...N4 (e)	0.88	2.27	3.038(5)	146
N4-H9...O18	0.87(6)	2.01(6)	2.865(5)	169(5)
O15-H15...N2 (f)	0.84	1.92	2.758(5)	173
O18-H18...N5 (d)	0.84	1.90	2.733(5)	169
C1-H1...O1	0.95	2.36	2.791(5)	107
C8-H8...O6	0.95	2.36	2.799(5)	107

S

Symmetry codes: (a) $-\frac{1}{2}+x, \frac{1}{2}+y, z$; (b) $\frac{1}{2}-x, \frac{1}{2}-y, -z$; (c) $x, 1+y, z$; (d) $1-x, 1-y, 1-z$; (e) $x, -1+y, z$;
(f) $x, y, 1+z$.